2001

Molecular Orbital Studies of Nitrosyl Metalloporphyrin Complexes

John P. Graham
Arkansas Tech University

Genevive Brown
Arkansas Tech University

Molecular Orbital Studies of Nitrosyl Metalloporphyrin Complexes

John P. Graham and Genevive Brown

Department of Physical Science, Arkansas Tech University, Russellville, AR 72801

Abstract

Molecular orbital calculations are applied to the study of the structure and bonding of nitrosyl metalloporphyrin complexes. The Fenske-Hall approximate molecular orbital method and the Amsterdam Density Functional (ADF) method are used. The calculations provide qualitative and quantitative explanations for the observed structural differences between the nitrosyl porphyrin complexes of iron, manganese, and cobalt. It is proposed that the energy of the highest occupied molecular orbital (HOMO) of these complexes is primarily responsible for the observed structural differences. The interaction between the nitrosyl ligand and metal d_z^2 orbital results in an antibonding orbital that is occupied in the complexes of Fe and Co, but unoccupied in the Mn complex. Bending of the metal-N-O linkage in complexes of Fe and Co results in stabilization of this orbital and consequently a more stable configuration for the complex. In addition, the binding affinity of these complexes for a sixth ligand is influenced by the energy and occupation of this largely metal-based orbital. The conclusions drawn from these calculations may provide evidence for the mechanism of activation of the enzyme soluble guanylyl cyclase, which is activated upon binding NO at metal porphyrin site.

Introduction

Nitric oxide, NO, is one of the most stable free radical molecules known. The biochemistry of NO has been a subject of much interest in recent years (Culotta and Koshland, 1992; Stamler et al., 1992; Feldman et al., 1993). NO plays an important role in many biological processes including neurotransmission, blood pressure regulation, and cytotoxic processes (Marletta, 1989; Ignarro, 1989; Ignarro, 1990; Garthwaite, 1991). NO also plays an important role in organometallic chemistry, where its ability to form stable complexes with odd electron metal fragments has led to the synthesis of many interesting molecules (Legzdins and Richter-Addo, 1988; Gladfelter, 1985; Griffith, 1968).

NO has been shown to activate the enzyme soluble guanylyl cyclase (sGC). sGC is an intracellular enzyme that catalyses the conversion of guanosine 5'-triphosphate to 3',5'-cyclic guanosine monophosphate (Waldman and Murad, 1987). It has been suggested that on binding NO at a heme group, an axial ligand is displaced from the heme group resulting in sGC activation (Traylor and Sharma, 1992; Dierks et al., 1997). Burstyn et al. (1994) have demonstrated through spectral evidence that an axial heme ligand is indeed displaced in sGC upon coordination of NO. The enzyme is also activated by cobalt nitrosyl porphyrins and the metal free co-factor PPIX (Ignaro et al., 1982; Ignarro et al., 1984). The enzyme is not activated by manganese nitrosyl porphyrin.

In this paper, MO calculations on metal nitrosyl porphyrin complexes of iron, manganese, and cobalt are presented. The principal focus of the paper will be that of the role of different metal centers in influencing the structure of the complexes and the binding affinity for a ligand trans to NO. The calculations lend support to the current models of activation of the enzyme sGC.

Methods

Fenske Hall calculations.--Fenske-Hall approximate molecular orbital calculations (Hall and Fenske, 1972) were carried out on a Pentium® based PC. All atomic basis functions were generated by a least squares fit of Slater-type orbitals to the atomic orbitals from Herman-Skillman atomic calculations (Bursten et al., 1978). Contracted double ζ representations were used for the Mn, Fe, Co 3d, and C, O, N 2p atomic orbitals. An exponent of 1.16 was used for the hydrogen 1s AO's (Hehre et al., 1969). The basis functions for Mn, Fe and Co were derived for the +1 oxidation state with 4s and 4p exponents of 2.0 and 1.8, respectively. The porphyrin ring used in all calculations was simple porphine $(C_{20}N_4H_{12})$ in which the 31 lowest and 40 highest lying molecular orbitals were deleted from the variational set of orbitals (all orbitals below the lowest π and above the highest π^* were deleted). The porphyrin ring was idealized for D_{4h} symmetry. The metal in all cases, unless otherwise specified, was placed 0.1 Å above the plane of the porphyrin ring. Imidazole (Im) was used as a model for histidine (His) in 6- coordinate complexes. The structure of imidazole was taken from the Alchemy molecular modeling program database. A N-O bond length of 1.176 Å was used for the nitrosyl ligand (Orpen et al., 1989). Metal-nitrosyl bond distances used were 1.646, 1.669 and 1.651 Å for Co, Fe, and Mn, respectively (Orpen et al., 1989). The 3σ and 6σ orbitals of NO were deleted from the set of variational orbitals.

Density functional calculations.--Density functional calculations were carried out on a Cray YMP supercomputer using the Amsterdam Density Functional program (Baerends et al., 1973). Double-ζ basis sets were used for C,

N and H of the porphyrin ring. A triple-ζ basis was used for N and O of NO, and Mn, Fe and Co. The $1s^2$ configurations of C, N and O and the $1s^2$, $2s^2$, $2p^6$ configurations of Mn, Fe and Co were treated as core. All calculations were carried out with Becke (1988) and Perdew (1986) non-local corrections. All bond distances and angles were those used in the Fenske-Hall calculations.

Results

The Metal-Porphyrin Interaction.--A brief summary of the Fenske-Hall picture of the metal porphyrin interaction is given here in order to identify the important frontier molecular orbitals used in the discussion of 5- and 6- coordinate complexes. The principal interactions involved in metal-
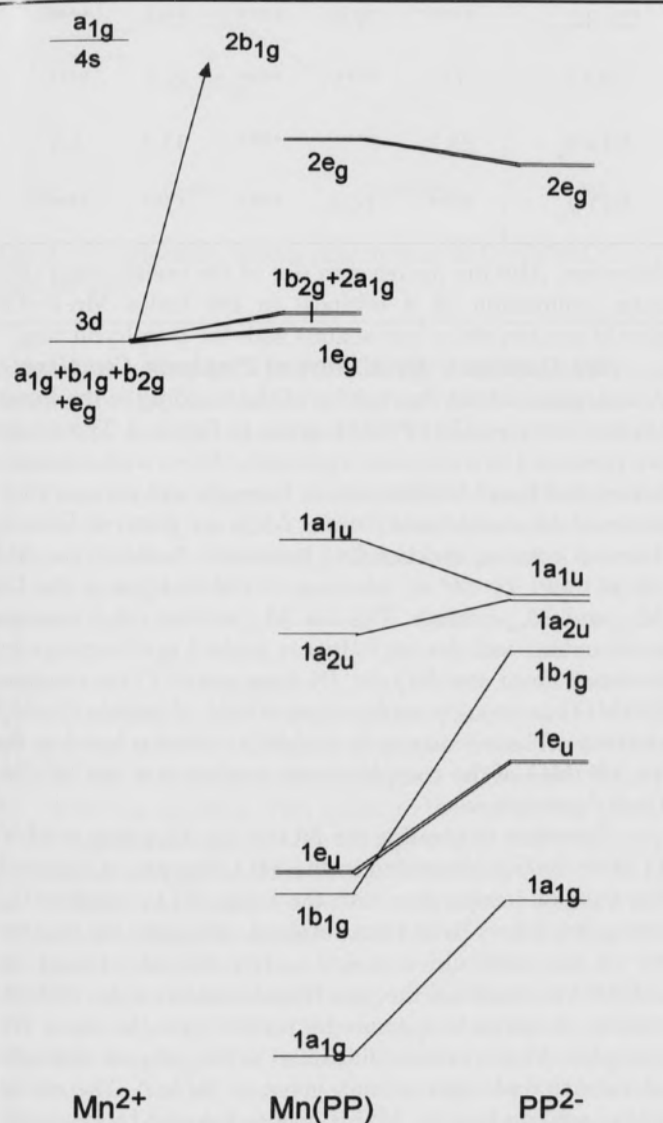

Fig. 1. A molecular orbital description of the Mn - porphyrin interaction

Table 1: Mulliken populations of frontier MOs in metal porphyrin complexes

	Mn	Fe	Co
Porphyrin a_{1g}	1.535	1.532	1.536
Porphyrin e_u (total)	3.276	3.264	3.252
Porphyrin b_{1g}	1.301	1.321	1.326
Porphyrin $2e_g$ (total)	0.378	0.280	0.190
Metal total	6.559	7.653	8.758
Metal total d	5.448	6.449	7.510
$3d_z^2$	0.126	0.101	1.017
$3d_{x^2-y^2}$	0.701	0.680	0.675
$3d_{xy}$	1.017	2.000	2.000
$3d_{xz}$	1.802	1.859	1.909
$3d_{yz}$	1.802	1.859	1.909
$4s$	0.342	0.370	0.449
$4p_x$	0.372	0.378	0.384
$4p_y$	0.372	0.378	0.384
$4p_z$	0.025	0.028	0.031

porphyrin bonding are illustrated in Figure 1. The molecular orbital diagram describes the combination of Mn^{2+} with a porphyrin^{2-} (PP^{2-}) ligand with the manganese atom in the plane of the porphyrin ring. The Mn $3d_{x^2-y^2}$ orbital, the lobes of which point towards the porphyrin N atoms, is pushed up in energy through interaction with the b_{1g} porphyrin orbital. The porphyrin also acts as an electron donor through the a_{1g} orbital (to manganese 4s) and e_u orbitals (to manganese p_x and p_y). The porphyrin $2e_g$ orbitals (Lowest Unoccupied Molecular Orbital (LUMO) of porphyrin^{2-}) interact with the metal d_{xz} and d_{yz} orbitals in a backbonding fashion. However, donation from the porphyrin $1e_g$ (not shown) results in an overall slight destabilization of the metal-based e_g (d_{xz}, d_{yz}) orbitals. The HOMO of MnPP is a singly occupied, essentially non-bonding, metal based orbital (b_{2g}). The LUMO of manganese porphyrin is the largely Mn $3d_z^2$ based non-bonding a_{1g} orbital. The electronic structure of iron porphyrin is similar; the HOMO is
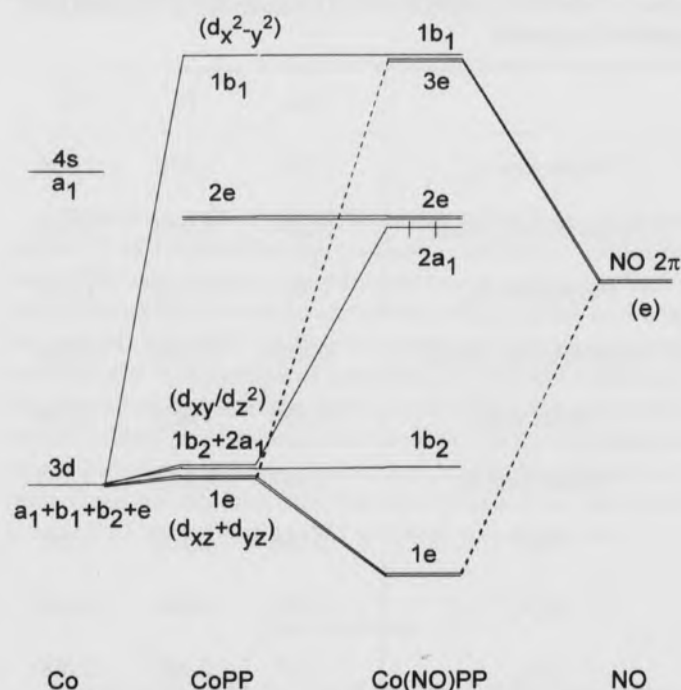
Fig. 2. A molecular orbital description of Co(PP)NO, linear NO

Table 2. Percent character and energy of valence MOs of Co(PP)NO, $\theta=180^{\circ}$ (**** <1%)

	2e	2e	1b$_2$	1a$_1$	1b$_1$
Energy (eV)	-9.36	-9.29	-8.32	-6.11	-3.43
Co $3d_z^2$	4.9	****	****	42.7	1.6
Co $3d_{x^2y^2}$	****	****	****	****	59.1
Co $3d_{xy}$	****	****	98.9	****	****
Co $3d_{xz}$	62.1	****	****	20.4	****
Co $3d_{yz}$	****	72.6	****	****	****
NO 5	1.0	****	****	6.3	****
NO 2_x	23.3	****	****	11.3	4.0
NO 2_y	****	18.9	****	****	****

a doubly occupied metal-based non-bonding b_{2g} orbital, and the LUMO is a nonbonding metal based a_{1g} orbital. In Co porphyrin the HOMO is a singly occupied a_{1g} orbital, and the LUMO is a porphyrin-based $2e_g$ orbital. Due to the closeness in energy of the metal-based valence MOs (e_g, a_{1g}, b_{2g}) of these complexes, no attempt is made to deduce a ground state configuration from these results. The ground state of iron porphyrin is largely believed to be $^3A_{2g}$, corresponding to the configuration $(d_{xy})^2(d_z^2)^2(d_{xz},d_{yz})^2$ (Sontum and Case, 1983). The $(d_{xz},d_{yz})^4(d_{xy})^2$ configuration ($^1A_{1g}$) predicted by the Fenske-Hall calculations is not unreasonable considering the similarity in energy of the metal frontier orbitals and the level of approximation inherent to these calculations.

Mulliken populations for some of the frontier orbitals of M^{2+} (M=Mn, Fe, Co) and PP^{2-} in the complexes MPP are given in Table 1. Clearly the additional electrons in the series MnPP, FePP, CoPP reside on the metal center. The variation of π and σ-interactions of the porphyrin with Mn, Fe, and Co is interesting: The degree of metal to porphyrin-$2e_g$ backbonding decreases from Mn-Fe-Co despite the increasing number of metal based electrons available for bonding. This can be attributed to the increasing energetic gap between the metal $d\pi$ orbitals and porphyrin $2e_g$ orbitals as the valence d orbital energy of successive metals

decreases. Also the decrease in size of the metal center (relative contraction of d orbitals) in the series Mn-Fe-Co should weaken the π interactions with the porphyrin ring.

Five Coordinate Metal Nitrosyl Porphyrin Complexes.-- A molecular orbital description of the bonding in the linear nitrosyl complex Co(PP)NO is given in Figure 2. The results are presented in a fragment approach, shown as the interaction of CoPP and NO fragments. Energies and percent characters of the metal-based frontier MOs are given in Table 2. There is a strong backbonding interaction between the NO 2π ($\pi*$) and Co $d\pi$ (e), resulting in stabilization of the Co $3d_{xz}$ and $3d_{yz}$ orbitals. The Co $3d_{xy}$ orbital (1b$_2$) remains nonbonding, and the $3d_z^2$ (1a$_1$) is pushed up in energy by donation from the NO 5σ (N lone pair). The resultant HOMO is a strongly antibonding orbital, of mainly Co $3d_z^2$ character. There exists no formal NO - metal σ bond as the 1a$_1$ HOMO of the complex is the antibond of the NO 5σ-Co d_z^2 interaction.

The effect of bending the NO in the XZ plane to M-N-O $(\theta) = 140^{\circ}$ is illustrated in the MO diagram of Figure 3. For ease of comparison with the linear NO complex, C_{4v} symmetry labels have been retained, although the symmetry of the molecule is now C_s. The Co $3d_z^2$ based 1a$_1$ HOMO is stabilized through backdonation to the NO $2\pi_x$ orbital, an interaction symmetry forbidden in the linear NO complex. This is clearly illustrated in the percent character of valence molecular orbitals given in Table 3. The energy of the antibonding 1a$_1$ MO is further lowered by decreased interaction with the NO 5σ orbital. These effects are accompanied by a decrease in NO $2\pi_x$-Co d_{xz} overlap (Table 4).
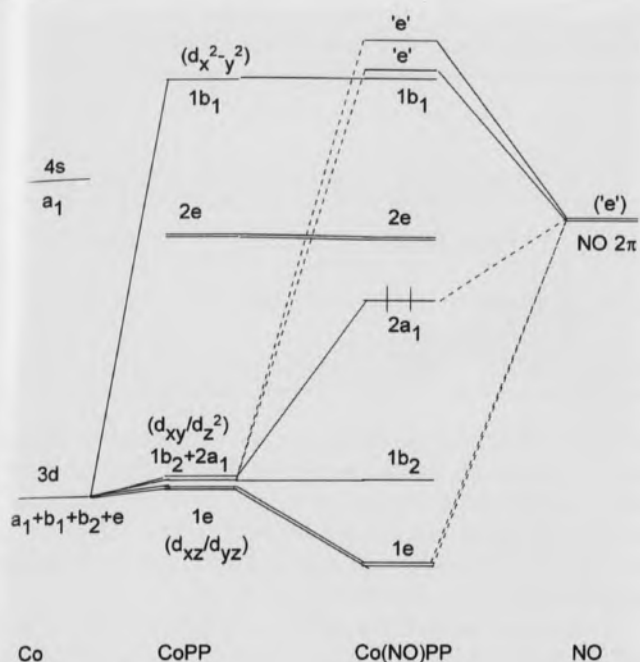
Journal of the Arkansas Academy of Science, Vol. 55, 2001

Fig. 3. A molecular orbital description of Co(PP)NO, NO bent ($\theta=140^\circ$)

Table 3. Percent character and energy of valence MOs of Co(PP)NO, $\theta=140^\circ$ (**** <1%)

	2e	2e	1b$_2$	1a$_1$	1b$_1$
Energy (eV)	-9.93	-9.93	-8.69	-5.68	-3.59
Co 3d$_z^2$	****	****	****	64.5	1.6
Co 3d$_{x^2y^2}$	****	****	****	****	62.1
Co 3d$_{xy}$	****	****	98.8	****	****
Co 3d$_{xz}$	64.5	****	****	****	****
Co 3d$_{yz}$	****	64.4	****	****	****
NO 5	****	****	****	4.3	****
NO 2$_x$	****	****	****	4.3	****
NO 2$_y$	****	23.8	****	****	****

Also the decrease in NO 5σ - Co d$_z^2$ overlap results in a decrease in stabilization of the NO 5σ - Co bonding molecular orbital (not shown, an increase in energy of ~0.85 eV is observed).

Considerable changes in the Mulliken populations for the Co dπ, NO 2π and Co d$_z^2$ orbitals are observed on bending (Table 3). The Co d$_z^2$ Mulliken population decreases on bending by ~0.36 due to d$_z^2$ → NO 2π_x back-bonding and decreased NO 5σ → d$_z^2$ σ donation. The populations of the Co d$_{xz}$ and d$_{yz}$ orbitals increase by 0.32 and 0.14 respectively. The change in d$_{xz}$ population is attributed to the decrease in d$_{xz}$ - NO 2π_x overlap on bending the nitrosyl and the newly introduced donation from the NO 5σ orbital. The NO 5σ population is seen to increase slightly (by ~0.05) on bending. This is due to the competing effects of decreased overlap with the Co d$_z^2$ orbital and the newly introduced interaction with Co d$_{xz}$. The change of +0.16 in the Mulliken population of the NO 2π_x orbital results from the back-bonding interaction with Co d$_z^2$, countering the decrease in donation from the Co d$_{xz}$. The increase in Mulliken population of the Co d$_{yz}$ orbital may at first seem odd as the Co d$_{yz}$ - NO 2π_y overlap is relatively unperturbed on bending NO (Table 4). However, we can attribute the change to the increased electron density on NO because of increased back-donation to the 2π_x orbital and decreased donation from the 5σ orbital. The decrease in population of the NO 2π_y orbital is consistent with the reduced donation

from Co d$_{yz}$. These results are qualitatively consistent with those derived from extended Hückel calculations on five coordinate organometallic metal nitrosyls (Hoffmann et al., 1974; Mingos, 1973).

A Walsh diagram for the valence molecular orbitals in CoPP(NO) on bending the nitrosyl ligand is given in Figure 4. On changing the Co-N-O angle from 180 to 120 degrees, we observe considerable stabilization of the 1a$_1$ HOMO and destabilization of the Co dπ based 1e orbitals. This is accompanied by a corresponding increase in HOMO-LUMO gap from 0.28 eV to 1.50 eV as the LUMO (porphyrin 2e$_g$) is essentially invariant in energy with θ. It is interesting to note that in this transformation from formal NO$^+$ ($\theta=180^\circ$) to formal NO$^-$ ($\theta=120^\circ$), we observe a flow of charge from metal to nitrosyl (Table 6). The difference in charge between linear NO and bent NO ($\theta=120^\circ$) is, however, only -0.128 e. Although consistent with the formal NO$^+$ → NO$^-$ direction of charge flow, the charges also suggest that the best description for NO, bent or linear, is an approximately neutral ligand. Contour plots, taken in the XZ plane, of the Co d$_{xz}$ and d$_z^2$ - NO interactions in bent ($\theta=140^\circ$) CoPP(NO) are given in Figure 5. The rehybridization of NO 2π_x / NO 5σ and Co d$_{xz}$/ Co d$_z^2$ are clearly evident. Figure 6 compares the interactions between NO and M in the bent and linear complexes M(PP)NO.

The degree of bending observed in a given complex will depend upon the relative effect of the above interactions
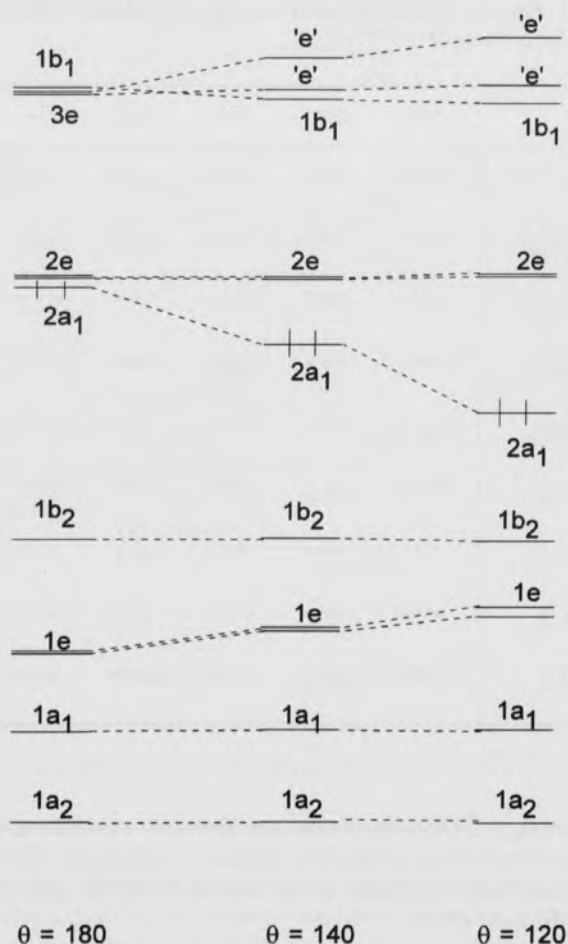
Fig. 4. Walsh diagram for the variation of frontier orbital energies of Co(PP)NO with θ

Table 4. Fenske-Hall calculated overlaps between Co and NO orbitals for linear and bent NO in CoPP(NO)

	NO 5σ	NO $2\pi_x$	NO $2\pi_y$
	Linear / Bent	Linear / Bent	Linear / Bent
Co $3d_z{}^2$	0.130 / 0.111	0.000 / 0.059	0.000 / 0.000
Co $3d_{xy}$	0.000 / 0.053	0.092 / 0.063	0.000 / 0.000
Co $3d_{yz}$	0.000 / 0.000	0.000 / 0.000	0.092 / 0.090

has shown the dihedral angle to vary considerably among similar systems, and a low barrier to rotation has been previously predicted (Hoffmann et al. 1974). For this discussion, the nitrosyl ligand will always be bent in the XZ plane as this simplifies the molecular orbital description by minimizing rehybridization of the M dπ orbitals.

A molecular orbital description of Fe(PP)NO (Fe-N-O = 140°) is given in Figure 7. The $1a_1$ metal based HOMO is stabilized through interaction with the NO $2\pi_x$ orbital, as observed in Co(PP)NO. However, in the case of Fe, the HOMO is only singly occupied. Consequently, stabilization of this orbital would be expected to have a lesser effect on the total energy of the complex relative to the stabilization of the HOMO of Co(PP)NO. Hence, it is predicted that the destabilization of Fe dπ orbitals will be more influential in determining the degree of bending than the corresponding orbitals in Co(PP)NO. Consequently, a larger value of θ is expected for Fe(PP)NO relative to Co(PP)(NO). This is consistent with experiment, which shows Co-N-O = 135° and Fe-N-O = 149° in Co(TPP)NO (Scheidt and Hoard, 1973) and Fe(TPP)NO (Scheidt and Frisse, 1974), respectively. It is noted that the HOMO of Fe(PP)NO lies closer to the porphyrin e_g orbitals than that of CoPP(NO), largely due to the higher energy of the Fe 3d orbitals relative to the 3d orbitals of Co. This results in a smaller HOMO-LUMO gap (at 140°) for FePP(NO) (0.37eV) compared to CoPP(NO) (0.76eV). Although calculations on the linear NO complex of Fe were non-convergent (due to accidental degeneracy of porphyrin e_g and $a_1(d_z{}^2)$ during SCF cycles), calculations on Fe(PP)NO at 140° and 180° were performed with deletion of the porphyrin e_g LUMO orbitals. This deletion allows the calculation to converge readily but eliminates backdonation from Fe to the porphyrin ring. Consequently, data from these calculations cannot be directly compared to the previous calculations. However, comparison of calculations in which the porphyrin e_g LUMO is deleted at M-N-O = 140° and 180° does reveal similar trends in frontier orbital populations to those observed for Co(PP)NO. As in the Co complex, the population of Fe $d_z{}^2$ decreases, accompanied by an
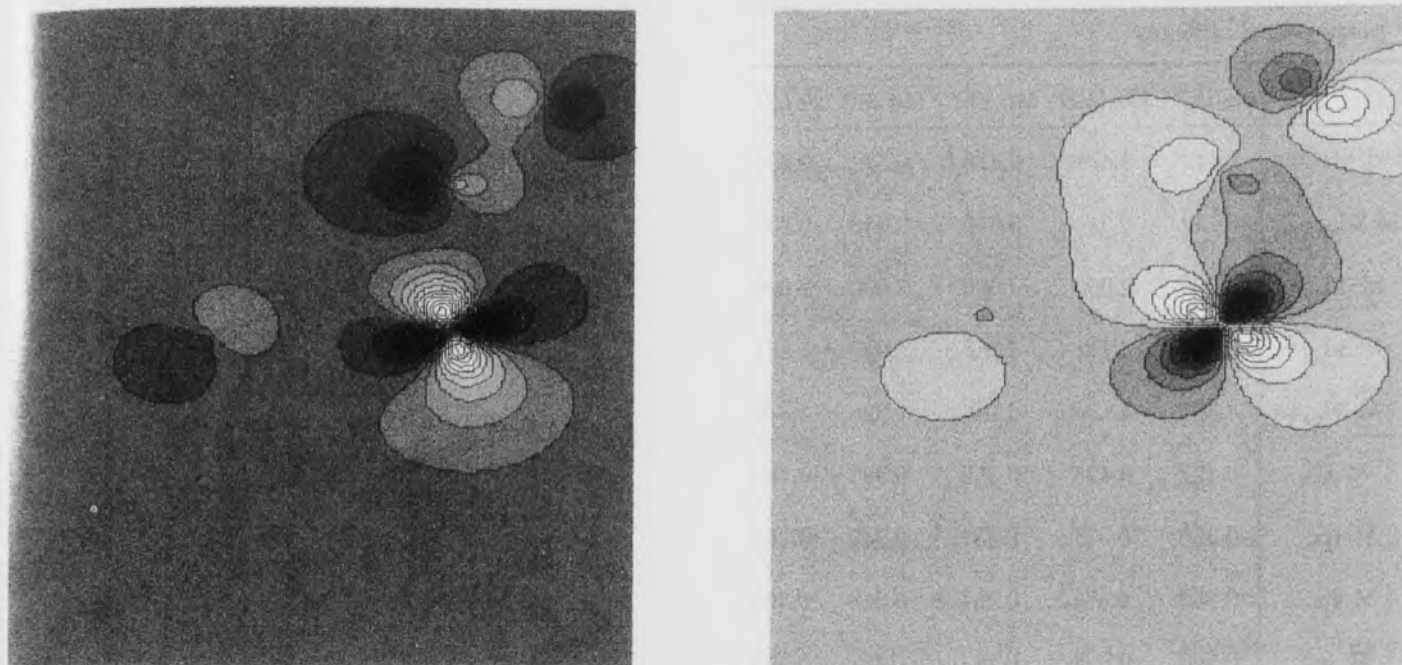
on the total energy of the complex. In the Walsh diagram of Figure 4, it is clear that the Co(PP)NO HOMO ($1a_1$) energy changes more rapidly with Co-N-O angle than the energy of the Co dπ (1e) orbitals. However, the dπ orbitals contain 4 electrons and consequently might be expected to contribute more to the total energy of the complex than the $1a_1$ HOMO. These factors will counter each other in determining the optimal Co-N-O angle.

It is also plausible for the Co-NO to bend at different dihedral angles to the XZ plane. The effect of bending the Co-NO at various dihedral angles to the XZ plane was investigated. No significant energetic difference between the different conformations was observed. The principal metal based valence MO's are essentially invariant with dihedral angle. No evidence was observed to suggest any direct interaction between the NO ligand and porphyrin ring at any dihedral angle. This is consistent with experiment, which

Fig. 5. Contour plots of the d_z2-NO and d_{xz}-NO interactions in bent Co(PP)NO

increase in the metal $d\pi$ populations, on bending the nitrosyl.

A molecular orbital diagram of Mn(PP)NO is given for Mn-N-O = 180° and Mn-N-O = 140° in Figure 8. The HOMO of Mn(PP)NO is a non-bonding metal based b_2 orbital (d_{xy}). The d_z^2 based $1a_1$ orbital is unoccupied, and therefore no stability is gained by introducing a NO2π - d_z^2 interaction on bending of the nitrosyl ligand. Therefore we predict bending of the nitrosyl ligand to be unfavorable, resulting in the destabilization of the metal $d\pi$ based e orbitals and reduced NO 5σ - Mn d_z^2 overlap.. The change in σ bonding is suggested to be the primary deterrent to bending in the Mn complex as decreased Mn d_{xz} - NO 2π_x overlap is compensated by mixing of the Mn d_z^2 orbital with d_{xz}, resulting in no significant change in energy of the $d\pi$ based e orbitals. The decrease in energy of the $1a_1$ d_z^2 / NO 5σ antibonding LUMO on bending is accompanied by a change of +0.73 eV in the energy of the largely NO 5σ based NO-Mn d_z^2 bonding MO. It is interesting to note that the Mn d_z^2 Mulliken population increases on bending. This may be attributed to NO 2π → d_z^2 donation, the opposite of the backdonation observed in the Fe and Co complexes. The Mn d_{xz} Mulliken population decreases on bending. Hence, electron density is effectively shuttled from the d_{xz} to d_z^2 orbital on bending NO, the opposite direction to that observed for the Fe and Co complexes.

Six-Coordinate Complexes.--Considering the above analysis of pentacoordinate metal porphyrin nitrosyls, the effect of a sixth ligand, trans to NO, can be readily discussed. A molecular orbital description of Mn(NO)PP(Im) (linear NO, Im = imidazole) is given in Figure 9. The occupied Mn 3d-based molecular orbitals are relatively unperturbed by the presence of imidazole. Imidazole acts primarily as a sigma donor ligand, with essentially no back-bonding ability. The Mn d_z^2 based a_1 orbital acts as an acceptor orbital for the imidazole N lone pair, resulting in stabilization of imidazole and destabilization of the virtual a_1 orbital. A net formal bond order of 1 is observed, and the HOMO-LUMO gap is unchanged. This interaction is favorable, stabilizing the Im lone pair and avoiding filled-filled orbital interactions while producing an 18-electron complex. Consequently, we would expect MnPP(NO) to form a stable bond to imidazole and similar ligands.

On interaction of Fe(PP)NO with imidazole, the singly occupied, largely d_z^2 based a_1 HOMO of Fe(PP)NO would be pushed up in energy, decreasing the HOMO-LUMO gap. This filled - half filled interaction would result in stabilization of the imidazole N lone pair, along with destabilization of the a_1 Fe(PP)(NO)(Im) HOMO. A formal bond order of 0.5 is predicted, consistent with the experimentally observed long Fe-(1-methyimidazole) bond in Fe(TPP)(NO)(1-MeIm) of 2.18 Å. (Scheidt and Piciulo, 1976).

Co(PP)NO is an 18-electron complex. Reaction of Co(PP)NO with imidazole would result in a filled-filled Co(PP)NO a_1-Im lone pair interaction. The largely d_z^2

Table 5. Mulliken populations in five-coordinate metal nitrosyl porphyrin complexes
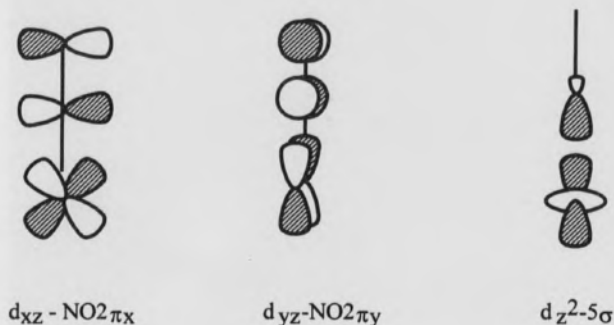
	Co 180°	Co 140°	Mn 180°	Mn 140°	Fe140°
M3d +NO2π	1.842	1.478	0.488	0.579	0.936
M $3d_{x2-y2}$	0.752	0.717	0.640	0.648	0.703
M $3d_{xy}$	2.000	2.000	2.000	2.000	2.000
M $3d_{xz}$	1.391	1.712	1.185	1.027	1.381
M $3d_{yz}$	1.391	1.526	1.185	1.228	1.419
M 4s	0.422	0.428	0.353	0.363	0.403
M $4p_x$	0.380	0.373	0.351	0.346	0.366
M $4p_y$	0.380	0.375	0.351	0.348	0.369
M 4p	0.568	0.398	0.184	0.176	0.269
M d total	7.376	7.433	5.498	5.482	6.439
M total	9.126	9.007	6.737	6.715	7.846
NO 5σ	1.630	1.683	1.553	1.584	1.630
NO $2π_x$	0.630	0.791	0.728	0.793	0.796
NO $2π_y$	0.630	0.474	0.728	0.682	0.552
M3d +NO2π	8.636	8.698	6.954	6.957	7.787

based antibonding a_1 HOMO of Co(PP)NO would be further destabilized by σ-donation from a trans ligand. No net bonding results (a formal bond order of 0, 20e complex); Co(PP)NO would not be expected to bind a sixth ligand.

These observations suggest that binding of NO to metalloporphryin complexes of Fe or Co will weaken or destroy bonding to a trans-σ-donor ligand. Binding of NO to a manganese metalloporphyrin complex will not significantly weaken a Mn-(trans-σ- donor) interaction. The proposed mechanism of activation of sGC by labilization of a distal ligand on binding NO is consistent with the above calculations and the observation of activation by Fe and Co nitrosyl porphyrins and the lack of activation by Mn nitrosyl porphyrins.

Total Energy Variations of M(PP)NO with M-N-O Angle.--Density functional calculations were performed to study the effect of M-N-O bending on the total energy of the

Linear M-NO interactions

$d_{xz} - NO2π_x$ $d_{yz}-NO2π_y$ $d_z{}^2-5σ$

Bent M-NO interactions

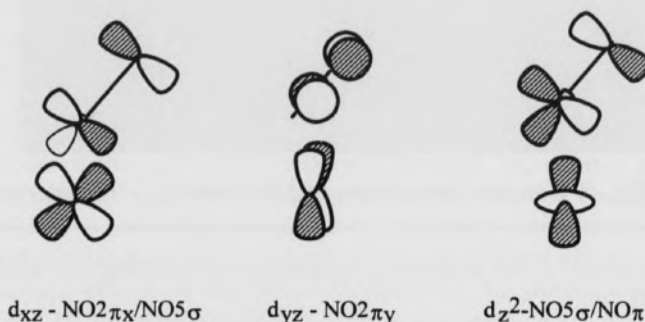$d_{xz} - NO2π_x/NO5σ$ $d_{yz} - NO2π_y$ $d_z{}^2-NO5σ/NOπ$

Fig. 6. Metal - nitrosyl bonding interactions in bent and linear M(PP)NO.

Table 6. Variation of charge distribution in Co(PP)NO with Co-N-O angle

θ	180°	140°	120°
Co	-.123	-.008	0.100
NO	0.156	0.111	0.028
Porphyrin	-0.033	-0.103	-0.128

complexes of interest. The Fenske-Hall results presented above suggest different degrees of bending for NO for Mn, Fe, and Co porphyrin nitrosyls. However, undermining these conclusions are two problems inherent to approximate Hartree-Fock methods. First, as approximations are made in calculation of the Fock matrix, the calculations are not truly variational. Therefore total energy comparisons are not
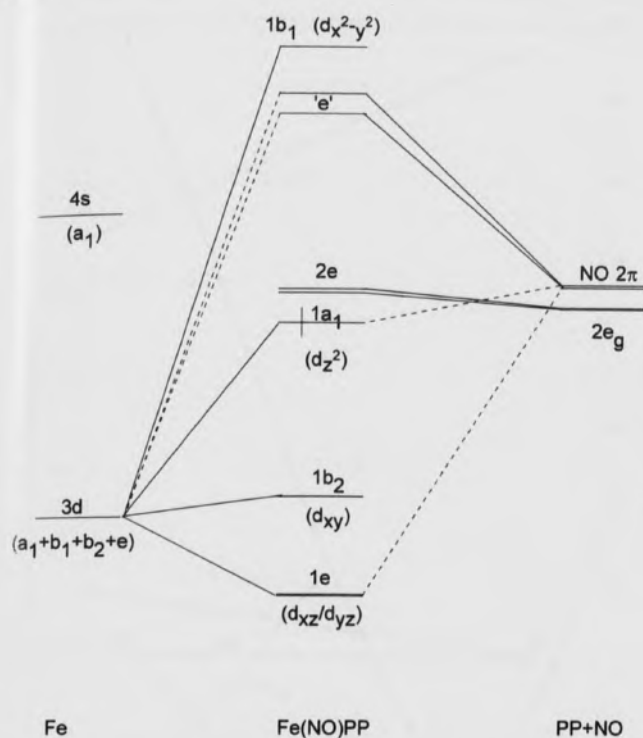
Fig. 7. A molecular orbital description Fe(PP)NO with $\theta = 140°$.

Fig. 8. Molecular orbital descriptions of Mn(PP)NO, NO bent and linear.

valid. Second, the arguments based upon the number of electrons stabilized and degree of stabilization may not be compelling. As the total energy is not simply the sum of the energies of occupied orbitals, this argument is open to criticism. Full energy minimization calculations on these metal porphyrin nitrosyl complexes would be prohibitively expensive due to the large number of functions and low (C_s) symmetry. Hence a series of single-point calculations at various M-N-O angles were carried out for the complexes M(PP)NO, M=Mn, Fe, and Co. Figure 10 shows the variation of total energy of the complexes M(PP)NO (M = Mn, Fe, Co) with M-N-O angle determined from a series of single point ADF calculations at the Becke-Perdew level. The porphyrin was idealized to D_{4h} symmetry, and the metal porphyrin complexes were given C_s symmetry (NO bent in the XZ plane). In each case, as in the Fenske-Hall calculations presented above, the metal was placed 0.10 Å above the plane of the porphyrin ring. The Co, Fe, and Mn complexes have energy minima at ~128°, 144°, and 180° respectively. The trend in optimal M-N-O angle is consistent with the Fenske-Hall results presented above.

The experimentally determined values θ, 135°, 149°, and ~176° for Co(TPP)NO (Scheidt and Hoard, 1973), Fe(TPP)NO (Scheidt and Frisse, 1975), and Mn(TPP)NO
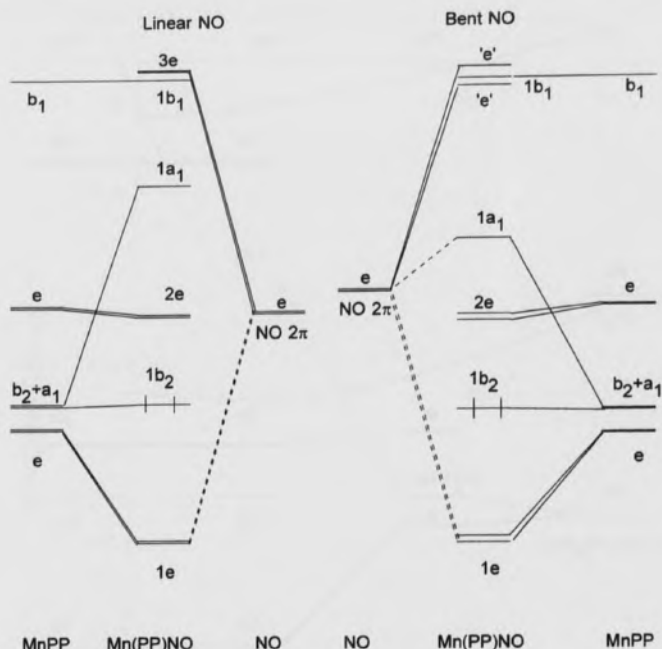
(Scheidt and Hoard, 1973) (TPP=tetraphenylporphyrin), respectively, indicate that the degree of bending is slightly overestimated in the ADF calculations. The agreement with experiment is, however, surprisingly good considering the approximations made in these calculations.

Figure 11 shows the variation of the energies of the $1a_1$ and $1e$ MOs with θ in Co(PP)NO. The variation of the $1a_1$ (HOMO) energy with θ is similar to that calculated by the Fenske-Hall method. The energetic variation of the Co $3d_{xz}$-based MO is consistent with the decrease in overlap between the NO $2\pi_x$ - Co d_{xz} orbitals on decreasing θ. The Co $3d_{yz}$-based MO is relatively invariant with θ, which is consistent with little or no change in overlap between NO $2\pi_y$ and Co d_{yz}. This differs somewhat from the Fenske-Hall results, where both the Co d_{xz} and d_{yz} changed considerably in energy with θ. The difference most probably arises from basis set effects and the fact that the net charge transfer between Co and NO on bending is considerably smaller in the ADF calculations.

The variation of NO charge with θ, including charges on the N and O atoms of NO, is illustrated in Figure 12. It is noted that the changes in the NO charge are dominated by changes in the charge on the N atom. This complements the description given earlier of the principal bonding changes with θ being controlled by the NO 5σ and NO 2π orbitals, both of which are largely based on the NO nitrogen
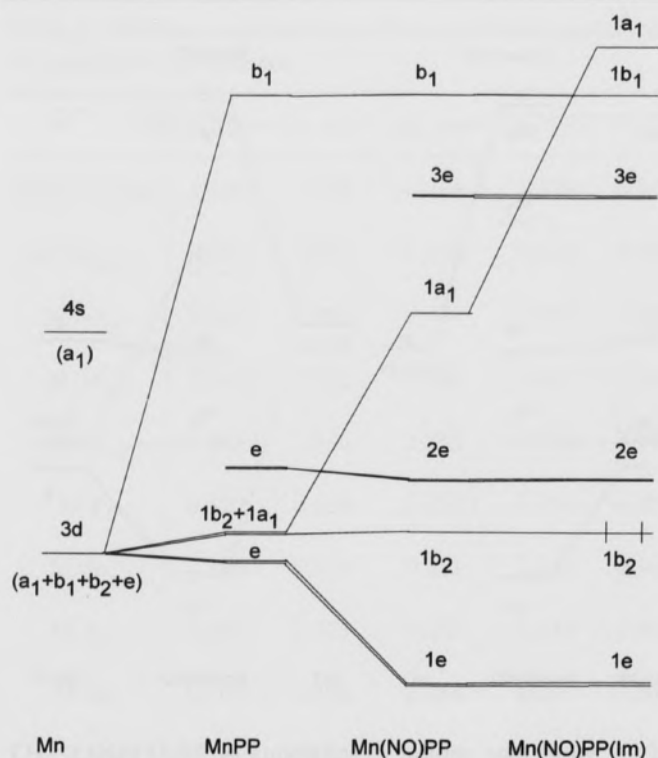
Fig. 9. A molecular orbital description of Mn(PP)(NO)Im.

Fig. 10. Variation of total energy of M(PP)NO (M = Mn, Fe, Co) with M-N-O angle.

atom. On bending, the NO ligand increases in total negative charge; this is consistent with the formal $NO^+ \rightarrow NO^-$ transformation. The calculated charge variations are very small and suggest, as noted before, that the best description of NO at any M-N-O angle in these complexes is that of an essentially neutral ligand.

Conclusions

The mechanism of activation of the enzyme sGC is believed to be related to the labilization of a His ligand trans to NO in a metal porphyrin group of the enzyme. The enzyme is activated by Fe and Co, but not by Mn. The results presented here suggest that labilization of the His residue is due to the localization of electron density in a metal d_z^2/NO 2π based orbital on going from Mn to Fe to Co. Further consistent with this is the observation that Fe(PP)(CO)(His) does not activate the enzyme. Fe(PP)CO is isoelectronic with Mn(PP)NO, and hence the a_1 (d_z^2) orbital is unoccupied. It is also predicted that Co(PP)CO, isoelectronic with Fe(PP)NO, would labilize a trans His ligand. The degree of bending of the nitrosyl ligand is dependent on the relative energy and occupation of the metal-based d_z^2 and $d\pi$ frontier orbitals. Our calculations predict a linear NO in MnPP(NO) and a bent NO in Fe(PP)NO and Co(PP)NO
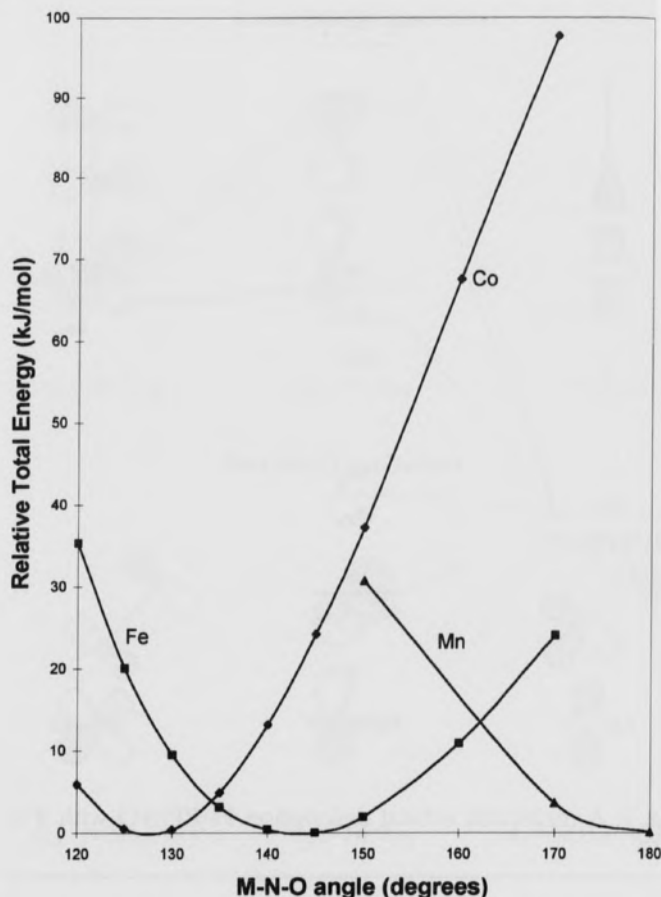
with M-N-O = 145° and 128°, respectively. These predictions are in good agreement with experimental values for M(TPP)NO complexes. The relative activation of the enzyme is also predicted to be greatest for Co(PP)NO, where 2 electrons reside in the antibonding a_1 HOMO.

Literature Cited

Baerends, E. J., D. E. Ellis, and P. Ros. 1973. Self consistent molecular Hartree-Fock-Slater calculations. I. Computational procedure. Chem. Phys. 2:41-51.

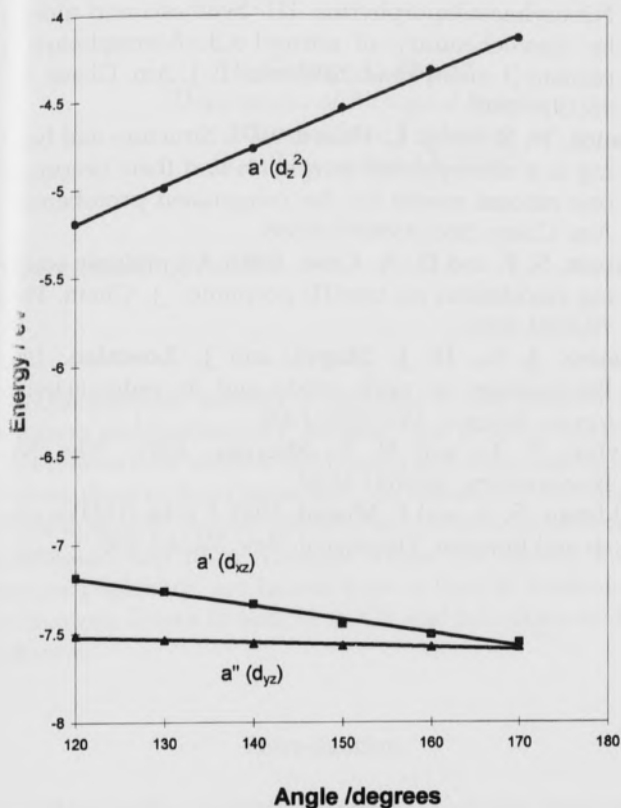Becke, A. D. 1988. Density functional exchange-energy

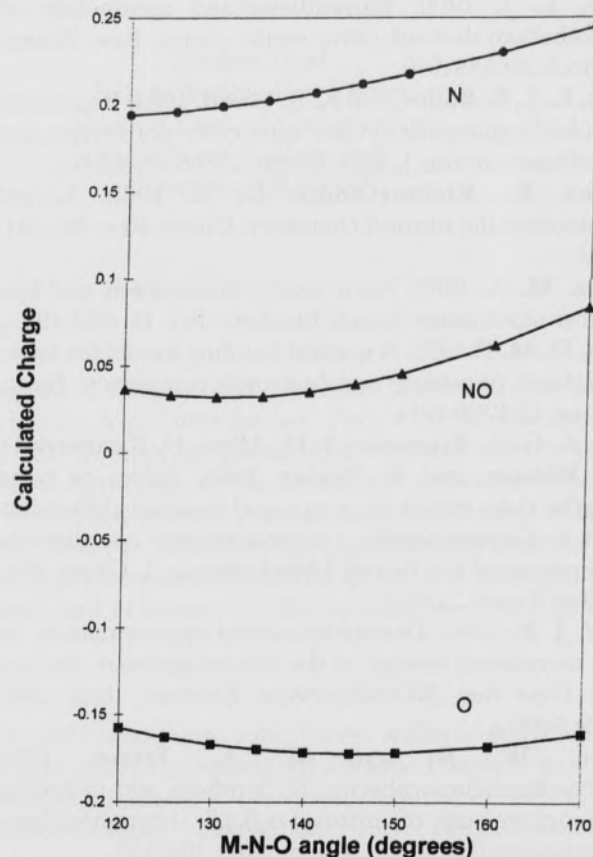Fig. 11. Energy variation of metal based frontier MOs with Co-N-O angle in Co(PP)NO

Fig. 12. Variation of NO charges with M-N-O angle in Co(PP)NO

approximation with correct asymptotic behavior. Phys. Rev. A38, 3098-3100.

Bursten, B. E., J. R. Jensen, and R. F. Fenske. 1978. An Xa optimized atomic orbital basis. J. Chem. Phys. 68, 3320-3321.

Burstyn, J. N., T. G. Spiro, S. Hu, and A. E. Yu. 1994. Resonance Raman spectroscopy of soluble guanylyl cyclase reveals displacement of distal and proximal heme ligands by NO. J. Am. Chem. Soc. 116: 4117-4118.

Culotta, E. and D. E. Koshland. 1992. NO news is good news. Science 258:1862-1865.

Dierks E. A., S. Hu, A. E. Yu, T. G. Spiro, and J. N. Burstyn. 1997. Demonstration of the role of scission of the proximal histidine-iron bond in the activation of soluble guanylyl cyclase through setalloporphyrin substitution studies. J. Am. Chem. Soc. 119: 7316-7323.

Feldman, P. L., O. W. Griffith, and D. J. Stuehr. 1993. The surprising life of nitric oxide. C&EN, December 20: 26-38.

Garthwaite, J. 1991. Glutamate, nitric oxide and cell-cell signaling in the nervous system Trends. Neurosci. 14: 60-67.

Gladfelter, W. L. 1985. Nitrosyl and Nitrido Metal Clusters Adv. Organomet. Chem. 24: 41-85.

Griffith, W. P. 1968. Organometallic nitrosyls. Adv. Organomet. Chem. 7: 211-239.

Hall, M. B. and R. F. Fenske. 1972. Electronic structure and bonding in methyl- and perfluoromethyl (pentacarbonyl)manganese. Inorg. Chem. 11: 768-775.

Hehre, W. J., R. F. Stewart, and J. A. Pople. 1969. Self-Consistent Molecular-Orbital Methods. I. Use of Gaussian Expansions of Slater-Type Atomic Orbitals. J. Chem. Phys. 51: 2657-2665.

Hoffmann, R., M., M. L. Chen, M. Elian, A. R. Rossi, and D. M. P. Mingos. 1974. Pentacoordinate nitrosyls. Inorg. Chem. 13:2666-2675.

Ignaro, L. J., K. S. Wood, and M. S. Wolin. 1982. Activation of purified soluble guanylate cyclase by protoporphyrin IX Proc. Natl. Acad. Sci. U.S.A. 79, 2970.

Ignarro, L. J. 1989. Heme-dependent activation of soluble guanylate cyclase by nitric oxide: regulation of enzyme activity by porphyrins and metalloporphyrins. Semin.

Hematol. 26: 63-76.

Ignarro, L. J. 1990. Biosynthesis and metabolism of endothelium-derived nitric oxide. Annu. Rev. Pharm. Toxicol. 30:535-560.

Ignarro, L. J., B. Ballot, and K. S. Wood. 1984. Regulation of soluble guanylate cyclase activity by porphyrins and metalloporphyrins J. Biol. Chem. 259:6201-6207.

Legzdins, P.; Richter-Addo, G. B. 1988. Recent organometallic nitrosyl chemistry. Chem. Rev. 88: 991-1010.

Marletta, M. A. 1989. Nitric oxide: biosynthesis and biological significance Trends Biochem. Sci. 14: 488-492.

Mingos, D. M. P. 1973. A general bonding model for linear and bent transition metal-nitrosyl complexes. Inorg. Chem. 12:1209-1211.

Orpen, A. G., L. Brammer, F. H. Allen, O. Kennard, D. G. Watson, and R. Taylor. 1989. Tables of bond lengths determined by x-ray and neutron diffraction. Part 2. Organometallic compounds and coordination complexes of the d- and f-block metals. J. Chem. Soc. Dalton Trans. S1-S83.

Perdew, J. P. 1986. Density-functional approximation for the correlation energy of the inhomogeneous electron gas. Phys Rev. B33:8822-8824. Erratum. Ibid. 1986. B34: 7406.

Scheidt, W. R. and M. E. Frisse. 1975. Nitrosylmetalloporphyrins. II. Synthesis and molecular stereochemistry of nitrosyl-$\alpha,\beta,\gamma,\delta$ -tetraphenylporphinatoiron (II). J. Am. Chem. Soc. 97:17-21.

Scheidt, W. R. and P. L. Piciulo. 1976. Nitrosylmetalloporphyrins. III. Synthesis and molecular stereochemistry of nitrosyl-$\alpha,\beta,\gamma,\delta$-tetraphenylporphinato (1-methylimidazole)iron(II). J. Am. Chem. Soc. 98:1913-1919.

Scheidt, W. R. and J. L. Hoard. 1973. Structure and bonding in a nitrosylcobalt porphyrin and their bearing on one rational model for the oxygenated protoheme. J. Am. Chem. Soc. 95:8281-8288.

Sontum, S. F. and D. A. Case. 1983. Xα multiple scattering calculations on iron(II) porphine. J. Chem. Phys. 79:2881-2892.

Stamler, J. S., D. J. Singel, and J. Loscalzo. 1992. Biochemistry of nitric oxide and its redox-activated forms. Science. 258:1898-1902.

Traylor, T. G. and V. S. Sharma. 1992. Why NO? Biochemistry, 31:2847-2849.

Waldman, S. A. and F. Murad. 1987. Cyclic GMP synthesis and function. Pharmacol. Rev. 39:163-196.